

## Persistence Lengths of DNA Obtained from Brownian Dynamics Simulations<sup>†</sup>

Steven P. Mielke,<sup>\*,‡</sup> Craig J. Benham,<sup>§</sup> and Niels Grønbech-Jensen<sup>||</sup>

NASA Goddard Institute for Space Studies, New York, New York 10025, UC Davis Genome Center, University of California, Davis, California 95616, and Department of Applied Science, University of California, Davis, California 95616

Received: December 07, 2008; Revised Manuscript Received: January 27, 2009

The persistence length of DNA has been studied for decades; however, experimentally obtained values of this quantity have not been entirely consistent. We report results from Brownian dynamics simulations that address this issue, validating and demonstrating the utility of an explicitly double-stranded model for mesoscale DNA dynamics. We find that persistence lengths calculated from rotational relaxation increase with decreasing ionic strength, corroborating experimental evidence, but contradicting results obtained from wormlike coil assumptions. Further, we find that natural curvature does not significantly affect the persistence length, corroborating cyclization efficiency measurements, but contradicting results from cryo-EM.

Important early measurements of the persistence length of DNA include those performed by Hagerman<sup>1,2</sup> and those performed by Rizzo and Schellman.<sup>3</sup> Reference 1 presents results of a Monte Carlo analysis that provides a quantitative relationship between rotational diffusion coefficients, as measured by optical anisotropy decay, and the persistence length of short, wormlike polymers. Reference 2 applies these results to observed rates of decay of birefringence for DNA restriction fragments ranging in size from 104 to 910 base pairs (bp) in solutions sampling a range of ionic strengths in both NaCl and MgCl<sub>2</sub>. The principal conclusion of refs 1 and 2 is that the persistence length of double-stranded DNA is not strongly dependent on ionic strength at concentrations above 1 mM NaCl, where its value is approximately 500 Å, but is significantly influenced by electrostatic contributions at lower concentrations. The onset of concentration insensitivity in MgCl<sub>2</sub> was seen to occur at a lower ionic strength than in NaCl. In ref 2, it is pointed out that the demonstrated ionic strength dependence underestimates that predicted by other investigators, and two possible explanations for this are proposed: (1) that electrostatic contributions to the excluded volume have not been correctly accounted for in studies using larger DNA molecules or (2) that the short chains used in the study reported in ref 2 do not manifest limiting (infinite chain length) polyelectrolyte behavior; i.e., the experimental results at low ionic strength may be influenced by finite-chain effects, which are discussed in more detail below.

In ref 3, Rizzo and Schellman report measurements on the flow dichroism of T7 DNA as a function of NaCl concentration. At high salt concentration, they find the persistence length to be 470 Å, which lies within the range 450–500 Å obtained by other methods, such as the aforementioned decay of electrically induced birefringence. As the salt concentration is decreased, they find that the persistence length begins to increase significantly near 5 mM, where the persistence lengths measured by Hagerman have leveled off to about 500 Å; i.e., the region where

Hagerman's results are essentially constant is where Rizzo and Schellman's results show a strong variation. To explain this discrepancy, the latter authors propose that the flexibility measured for the approximately 40 000 bp T7 DNA is affected by longer-range contributions to the excluded volume than are present in the short fragments employed by Hagerman.

In contradistinction to these results, other studies employing transient electric birefringence or dichroism have found that the persistence length decreases weakly with increasing ionic strength between 0.3 and 100 mM.<sup>4,5</sup> Moreover, studies employing light scattering,<sup>6,7</sup> flow birefringence,<sup>8</sup> and magnetic birefringence<sup>9</sup> have demonstrated a strong dependence of the persistence length on ionic strength at all salt concentrations, which is inconsistent with the much smaller dependence observed with transient electric birefringence or dichroism.

Investigations of the persistence length of DNA have also sought to quantify the relative contribution of its static and dynamic components. The former refers to the effect of sequence-dependent intrinsic curvature, and the latter to that of thermal fluctuations.<sup>10</sup> Results in this regard have been inconsistent. For example, in ref 11, Bednar et al. report on cryo-electron microscopy experiments indicating persistence lengths of around 500 Å for natural ("random"-sequence) molecules and 800 Å for intrinsically straight molecules, suggesting a static persistence length of around 1300 Å. This finding is contradicted by measurements of the cyclization efficiency of DNA fragments, reported by Vologodskia and Vologodskii in ref 12, indicating a persistence length of between 480 and 500 Å for both natural and intrinsically straight molecules, and therefore a negligible contribution from intrinsic curvature.<sup>12</sup> To our knowledge, this discrepancy has yet to be resolved.

Collectively, the foregoing clearly illustrate the extreme sensitivity of persistence length measurements to the molecules being considered, the experimental method being performed, and the model being employed to interpret the empirical results.

To validate and demonstrate the utility of the model presented in ref 13, we have measured DNA persistence lengths from Brownian dynamics simulations performed at salt concentrations spanning several orders of magnitude, and compared with some of the experimental results discussed above. The data presented here suggest the model can potentially address the inconsisten-

<sup>†</sup> Part of the "George C. Schatz Festschrift".

<sup>\*</sup> To whom correspondence should be addressed.

<sup>‡</sup> NASA Goddard Institute for Space Studies.

<sup>§</sup> UC Davis Genome Center.

<sup>||</sup> University of California.

cies characterizing these results. This model seeks to simulate physiologically relevant DNA dynamics, while preserving critical biological details—such as DNA double-strandedness and base identity, and the discreteness of ambient ions—omitted from most, if not all, mesoscale models designed for the same purpose. These simulations are predicated on a model described in detail in ref 13 and extend results presented therein. To summarize, double-stranded DNA is represented as two interwound chains of negatively charged Stokes spheres (beads), and ions as free, positively or negatively charged Stokes spheres. Intrachain particles within the DNA interact via elastic stretching and bending potentials characterized by force constants appropriate for single-stranded DNA. Interchain particles interact via a hydrophobic potential that incorporates base pairing and stacking energetics, allowing the model to capture phenomena, such as superhelical stress-induced DNA duplex destabilization, that depend sensitively on base sequence.<sup>14</sup>

In addition to these potentials specific to particles comprising the DNA, all particles interact via an excluded volume potential that prevents interparticle penetrations, and an electrostatic potential based on the Lekner summation strategy, which evaluates Coulomb forces and energies in periodic lattices with rectangular unit cells.<sup>15</sup> This strategy allows the model to represent a solution environment in which the polyions (DNA molecules) interact both with one another (periodic images of the molecule occupying the unit cell) and with explicitly represented salt species of specified concentration. Here, as in ref 13, the DNA was approximately 500 Å in length (representing 147 bp), and all ions were monovalent, making the solutions 1:1 in electrolytes. For a detailed description of this model, refer to refs 13 and 14.

Simulations were performed at 11 different salt concentrations, ranging from 0 to 100 mM, set by varying the volume of the simulation box and choosing an appropriate number of counterions and coions. In addition to the ions required to establish a bulk concentration of salt (the concentration that would exist in the absence of macroions), 294 counterions were included in each case to satisfy the electroneutrality condition, i.e., to neutralize the  $-294e$  net charge associated with the 147 bp DNA molecule, where  $e$  is the elementary charge. The smallest (zero salt) system then consisted of 394 particles ( $2N = 100$  beads representing the DNA and 294 representing neutralizing counterions) in a  $(1200 \text{ \AA})^3$  box, and the largest (100 mM salt) system consisted of 5394 particles (100 beads representing the DNA, 2500 representing coions, and  $2500 + 294 = 2794$  representing counterions) in a  $275 \times 275 \times 550 \text{ \AA}^3$  box. We note that the optimality of using a  $(1200 \text{ \AA})^3$  box in the former case, where the Debye length is effectively infinite, was not investigated. Subsequent to equilibration, on the order of  $10^7$  configurations of each of the 11 systems were generated using a Brownian dynamics algorithm.<sup>13,14,16</sup>

To calculate persistence lengths from the simulation results, two different strategies were employed. First, so that we could directly compare with the experimental results of Hagerman, following the procedure described in ref 13, we used the expression<sup>1</sup>

$$R_a = \tau_a/\tau_B = 1.0120 - 0.24813X + 0.033703X^2 - 0.0019177X^3 \quad (1)$$

Here,  $\tau_a/\tau_B$  is the ratio of the approximate rotational relaxation time to the Broersma rotational relaxation time, and  $X = L/P$ , where  $L$  is the molecular contour length (we used the value

500 Å, the total length of the double-chain central axis) and  $P$  is the persistence length. For a detailed discussion of the expressions for  $\tau_a$  and  $\tau_B$  and of the procedure used to calculate persistence lengths from rotational relaxation, see ref 13 and citations therein. Briefly,  $\tau_B$  was obtained from Broersma's empirically motivated relaxation time<sup>17</sup> using parameter values consistent with the simulations, and  $\tau_a$  was obtained from the relaxation time of Garcia de la Torre and Bloomfield<sup>18</sup> by calculating average values of the rotational diffusion coefficients from the simulation trajectories. For each simulation, with  $\tau_a$  and  $\tau_B$  determined, eq 1 was solved for  $P$ .

The second strategy employed to calculate persistence lengths was to use the familiar expression for wormlike chains:<sup>19,20</sup>

$$\langle \cos \theta \rangle = \exp(-L/P) \quad (2)$$

where  $L = 500 \text{ \AA}$  is again the molecular contour length and  $\theta$  is the angle between the tangents to the duplex axis end points. For these tangents, we used the vectors describing the first and last axis segments,  $a_1 = (r_2 - r_1)/|r_2 - r_1|$  and  $a_{N-1} = (r_N - r_{N-1})/|r_N - r_{N-1}|$ , where  $r_i$  is the position of the  $i$ th axis vertex or end point, defined as the midpoint between the  $i$ th pair of complementary beads in the double-chain. We then calculated  $\cos \theta \equiv (a_1 \cdot a_{N-1})/(|a_1||a_{N-1}|)$  for each system configuration and averaged over the same eleven simulation trajectories used to obtain persistence lengths from rotational diffusion data. Finally, with values of  $\langle \cos \theta \rangle$  determined, eq 2 was solved in each case for  $P$ .

The results of these persistence length calculations are shown in Figure 1, where persistence lengths in Ångstroms are plotted against the eleven molar salt concentrations characterizing the simulations. Figure 1a includes log-scale concentrations from 0.025 to 100 mM, and Figure 1b linear-scale concentrations from 0 to 0.1 mM. The vertical axis is log-scale in both parts of the figure. Persistence length values represented by filled triangles correspond to the rotational diffusion calculations, and those represented by open circles to the wormlike chain calculations. Between 0.5 and 100 mM, the former are in approximate agreement with the generally accepted value for B-DNA of 450–500 Å (we note that the 1, 10, and 100 mM data reproduce results reported in ref 13). However, at concentrations less than 0.5 mM, values of the persistence length calculated from rotational diffusions increase with decreasing concentration, as anticipated from previous results,<sup>13</sup> reaching the value  $43\,479 \pm 1153 \text{ \AA}$  at 0.025 mM, and  $144\,000 \pm 19\,000 \text{ \AA}$  at 0 mM. We note that the value at 0.1 mM ( $P = 10\,219 \pm 37 \text{ \AA}$ ) differs from that reported for the same concentration ( $P = 4709 \pm 15 \text{ \AA}$ ) in ref 13, where fewer system configurations were considered for purposes of calculating  $\tau_a$ . It can be seen in Figure 1 that persistence length values obtained from the wormlike chain calculations fluctuate little over the entire 100 mM domain of ionic strengths considered (the value at zero salt is  $1113 \pm 7 \text{ \AA}$ ). The mean of these values is  $1222 \text{ \AA}$ —more than twice the commonly assumed value for B-DNA.

Our diffusion-based results are in approximate agreement with the aforementioned experimental results of Hagerman<sup>2</sup> (shaded squares in Figure 1), which indicate values of the persistence length near 500 Å above approximately 0.5 mM, and a significant increase in the persistence length with decreasing concentration below 0.5 mM, reaching a value near 1800 Å at 0.1 mM. Similarly, our results (Figure 1) show a persistence length near 500 Å at concentrations of 0.5 mM and above, and an increase in the persistence length with decreasing concentration below 0.5 mM. We point out that Hagerman's data are

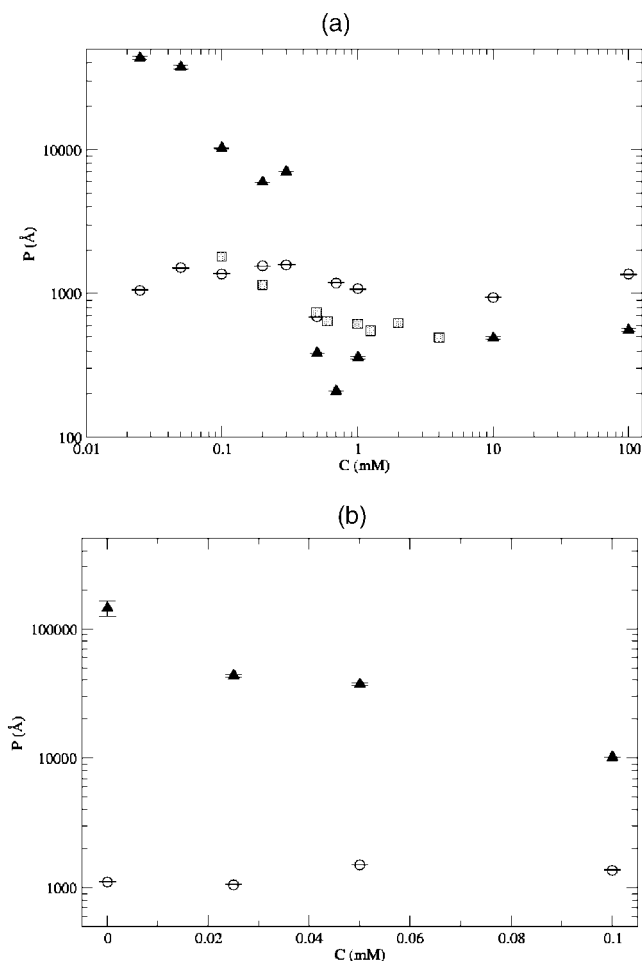


**Figure 1.** Persistence length vs salt concentration. Mean values of the persistence length and their standard deviations, calculated from simulations at eleven salt concentrations using expressions based on rotational diffusion (filled triangles) and wormlike chain assumptions (open circles). (a) Values calculated at zero salt are not shown, because both axes are log scale. Experimental data from ref 2, Figure 14, are included (shaded squares). (b) Data points for the case of zero salt— $144\,000 \pm 19\,000$  Å (diffusion) and  $1113 \pm 7$  Å (wormlike chain)—are included; ordinate is log scale.

suggestive of a more subtle onset of increase at a slightly higher concentration (our values increase sharply between 0.3 and 0.5 mM). We also point out that our values of the persistence length at low concentrations are significantly larger than Hagerman's (our value at 0.1 mM is again  $10\,219 \pm 37$  Å). These differences are perhaps a reflection of the previously mentioned model dependence of persistence lengths calculated from electro-optical relaxation times,<sup>21,22</sup> but they may also simply reflect limitations inherent to the dynamic model, e.g., inability of the simulations accurately to account for dielectric solvent effects (a constant value of the permittivity was assumed for purposes of calculating electrostatic interactions).

As mentioned above, the experimental results of Rizzo and Schellman (see Figure 5 in ref 3) show the onset of ionic strength dependence of the persistence length to occur at a concentration of around 5 mM—significantly larger than the values indicated by either Hagerman's data or the simulation results. In ref 23, Hagerman explores the possibility that this discrepancy is a consequence of finite-chain effects inherent to the relatively short DNA fragments used in his study, specifically, that electrostatic end effects influence apparent values of the persistence length under conditions in which its electrostatic component predominates. (Electrostatic end effects refer to

reduced flexural forces on finite chains, relative to infinite chains, due to diminished electrostatic self-repulsion (see also, e.g., ref 24). By performing an analysis based on the theoretical work of Skolnick and Fixman,<sup>25</sup> Hagerman derives a relationship between the apparent persistence length of a wormlike polyion and  $L$ , its reduced contour length, concluding that this is indeed the case; at least qualitatively, his experimental results can be interpreted in terms of a reduced electrostatic contribution to the persistence length for short DNA molecules, owing to electrostatic end effects.

If finite-chain effects also explain the discrepancy between the diffusion-based simulation results and Rizzo and Schellman's results (demonstrating this would require performing simulations involving longer molecules), Figure 1 suggests that persistence lengths calculated using eq 2 are even more sensitive to these effects than those calculated using eq 1; i.e., they evince no apparent dependence on ionic strength, even at zero salt. Visual inspection of the simulation trajectories reveals that the ends of the model DNA undergo spatial fluctuations significantly larger than those of interior regions, as anticipated from mechanical considerations. Because only the terminal segments of the molecular axis are used to calculate  $\cos \theta$  in eq 2, effects of these local motions dominate those of any global stiffening, and the method underestimates ionic strength dependence of the persistence length even moreso than that based on rotational diffusion, which considers the entire structure. At least in the nonlimiting (finite-length) case, then, these two definitions of the persistence length predict fundamentally different behaviors of the polyion, indicating that caution should be exercised in their application. Inasmuch as real polyions in solution likely experience these disproportionate end motions, it may be that expressions based only on terminal orientations, such as eq 2, are generally incapable of accurately characterizing polymer conformational properties *in vivo*. We point out that an additional conclusion of ref 23 is that, unless  $L \gg 1$ , analyses at low ionic strengths should ideally specify persistence length as a function of position along the molecular contour, which suggests a potential area of future investigation for the methods reported here.

It is also evident from Figure 1 that values of the persistence length from eq 2 are larger than those from eq 1 in the regime of high salt concentrations; as mentioned above, the average of the former is more than twice the commonly assumed value of 500 Å. As we have seen, the persistence length calculations based on wormlike coil assumptions are sensitive predominantly to dynamic end effects, so these do not likely provide an accurate measure of the overall bending stiffness of the model polyelectrolyte. However, as noted previously, the apparent persistence length of intrinsically straight DNA might exceed 500 Å if intrinsic curvature makes a substantial contribution to the apparent persistence length of natural DNA. The findings reported in ref 11 suggest this is the case but are contradicted both by the findings reported in ref 12 and by our diffusion-based calculations from the simulation results, which yield persistence lengths of around 500 Å for the intrinsically straight model fragments at concentrations where electrostatic contributions are expected to be small.

Calculation of persistence lengths from experimental data is generally very model-dependent. For example, Hays et al. have noted that persistence lengths calculated from light scattering and hydrodynamic data differ by as much as 50%.<sup>26</sup> More recently, Manning has discussed the previously mentioned discrepancy between results indicating a significant dependence of the persistence length on ionic strength, even at high salt



concentrations, and those from transient electric birefringence and dichroism indicating a much smaller dependence.<sup>27</sup> Specifically, in ref 27, Manning introduces a “null isomer” DNA model that corroborates the former results and critiques models of the aforementioned Odijk–Skolnick–Fixman type<sup>25,28</sup> on the grounds that they are predicated on unrealistic assumptions, namely, that the polymer structure is invariant to changes in electrostatic forces. (We note that, because the DNA structure in our model responds dynamically to changes in electrostatic forces, the discrepancy between our results and Manning’s at moderate salt concentrations, where our diffusion-derived values are approximately constant, warrants further investigation.) For an assessment of various theoretical approaches to the electrostatic persistence length within the Debye–Hückel approximation, see ref 29.

Model sensitivity of the persistence length has also been demonstrated by Seol and co-workers, who have recently discussed length dependence, and introduced a finite wormlike chain model that improves upon the classical (limiting) model for purposes of analyzing data from single-molecule experiments.<sup>30</sup> The framework presented here further highlights the importance of model choice in calculating persistence lengths by predicting two qualitatively and quantitatively different results based on the same data set. This framework may provide a means for exploring this issue in detail in a dynamic and quasi-physiological context.

In conclusion, persistence length is evidently a highly variable measure of the bending stiffness of DNA, sensitive not only to physical properties of the molecule under consideration (e.g., its length and mechanical behaviors) and its electrolytic environment but also to the empirical and theoretical methodologies employed to obtain it. Here, we have reviewed experimental results that illustrate this variability, indicating that apparent persistence length varies with ionic strength in a manner that depends on polyion length (excluded volume and end effects), experimental method, and model and may or may not be affected by intrinsic curvature in natural DNA sequences. Additionally, we have reported results from Brownian dynamics simulations that corroborate some of these findings and contradict others, indicating that apparent persistence length might be influenced by local dynamics within finite chains but may not be affected by intrinsic curvature. The former potentially has implications for the extent of validity of a commonly used expression for persistence length based on wormlike chain assumptions (i.e., eq 2). Persistence lengths calculated from the simulations using this expression suggest behavior of the polyion (no stiffening

even at very low ionic strength) that is dramatically different both from that suggested by calculations using eq 1 and from what is seen experimentally. Taken together, these results indicate that the model described in ref 13 can potentially provide insight on open questions in this area. Future studies designed for this purpose should further investigate, for example, polyion length dependence and salt valency dependence of electrostatic contributions to persistence length measurements.

**Acknowledgment.** We acknowledge the contributions of Professors William H. Fink and Krish V. Krishnan.

## References and Notes

- (1) Hagerman, P.; Zimm, B. *Biopolymers* **1981**, *20*, 1481.
- (2) Hagerman, P. *Biopolymers* **1981**, *20*, 1503.
- (3) Rizzo, V.; Schellman, J. *Biopolymers* **1981**, *20*, 2143.
- (4) Porschke, D. *Biophys. Chem.* **1991**, *40*, 169.
- (5) Lu, Y.; Weers, B.; Stellwagen, N. C. *Biopolymers* **2002**, *61*, 261.
- (6) Borochov, N.; Eisenberg, H.; Kam, Z. *Biopolymers* **1981**, *20*, 231.
- (7) Sobel, E. S.; Harpst, J. A. *Biopolymers* **1991**, *31*, 1559.
- (8) Cairney, K. L.; Harrington, R. E. *Biopolymers* **1982**, *21*, 923.
- (9) Maret, G.; Weill, G. *Biopolymers* **1983**, *22*, 2727.
- (10) Trifonov, E. N.; Tan, R. K. Z.; Harvey, S. C. In *Structure & Expression*; Olson, W. K., Sarma, M. H., Sarma, R. H., Sundaralingam, M. S., Eds; Adenine Press, Inc.: Albany, NY, 1988.
- (11) Bednar, J.; et al. *J. Mol. Biol.* **1995**, *254*, 579.
- (12) Vologodskaja, M.; Vologodskii, A. *J. Mol. Biol.* **2002**, *317*, 205.
- (13) Mielke, S. P.; Grønbech-Jensen, N.; Benham, C. J. *Phys. Rev. E* **2008**, *77*, 031924.
- (14) Mielke, S. P.; Grønbech-Jensen, N.; Krishnan, V. V.; Fink, W. H.; Benham, C. J. *J. Chem. Phys.* **2005**, *123*, 124911.
- (15) Grønbech-Jensen, N. *Int. J. Mod. Phys. C* **1997**, *8*, 1287.
- (16) Mielke, S. P.; Fink, W. H.; Krishnan, V. V.; Grønbech-Jensen, N.; Benham, C. J. *J. Chem. Phys.* **2004**, *121*, 8104.
- (17) Broersma, S. J. *J. Chem. Phys.* **1960**, *32*, 1626.
- (18) Garcia de la Torre, J.; Bloomfield, V. A. *Biopolymers* **1977**, *16*, 1765.
- (19) Landau, L. D.; Lifshitz, E. M. *Statistical Physics, Course of Theoretical Physics*; Pergamon: London, 1958.
- (20) Bloomfield, V. A.; Crothers, D. M.; Tinoco, I., Jr. *Nucleic Acids: Structures, Properties, and Functions*; University Science Books: Sausalito, CA, 2000.
- (21) Elias, J. G.; Eden, D. *Macromolecules* **1981**, *14*, 410.
- (22) Hagerman, P. *Annu. Rev. Biophys. Biophys. Chem.* **1988**, *17*, 265.
- (23) Hagerman, P. J. *Biopolymers* **1983**, *22*, 811.
- (24) Anderson, C. F.; Record, M. T., Jr. *Annu. Rev. Phys. Chem.* **1995**, *46*, 657.
- (25) Skolnick, J.; Fixman, M. *Macromolecules* **1977**, *10*, 944.
- (26) Hays, J. B.; Magar, M. E.; Zimm, B. H. *Biopolymers* **1969**, *8*, 531.
- (27) Manning, G. S. *Biophys. J.* **2006**, *91*, 3607.
- (28) Odijk, T. *J. Polym. Sci., Polym. Phys. Ed.* **1977**, *15*, 477.
- (29) Ullner, M. *J. Phys. Chem. B* **2003**, *107*, 8097.
- (30) Seol, Y.; et al. *Biophys. J.* **2007**, *93*, 4360.